ADVANCED FUNCTIONAL MATERIALS
www.afm-journal.de

The Influence of A-Site Rare Earth Ion Size in Controlling the Curie Temperature of $Ba_{1-x}RE_xTi_{1-x/4}O_3$

Colin L. Freeman, James A. Dawson, John H. Harding, Liu-Bin Ben, and Derek C. Sinclair*

The defect structures for Gd- and La-doping on the A-site of $BaTiO_3$ with the creation of Ti vacancies are reported. The rare-earth cations cluster together around the vacancy. The local relaxations caused by the defect cluster lead to distortion and tilting of nearby TiO_6 octahedra and this is responsible for the lowering of the Curie temperature with increasing dopant concentration. Larger distortions to the octahedra are observed for La-doping and this is the proposed origin of the greater decrease in T_c as observed by experimental results associated with La- compared to Gd-doped samples.

1. Introduction

Ferroelectric $BaTiO_3$-based materials are the cornerstone of the electroceramics market and find applications as high permittivity dielectrics in multilayer ceramic capacitors and as non-ohmic ceramics that exhibit a positive temperature coefficient of resistance for temperature sensors and current overload protection devices.[1–3] $BaTiO_3$ is the archetypal ferroelectric (ABO_3) perovskite and the ferro- to para-electric phase transition from tetragonal (space group *P4mm*) to cubic symmetry (space group *Pm3m*) occurs at ≈120–130 °C and is known as the Curie Temperature, T_c. In many applications, control of T_c is required and this is commonly achieved via chemical doping, either on the A- and/or B-site.[4] To improve device performance and future applications of $BaTiO_3$ or related ABO_3 ferroelectrics it is important to understand the defect chemistry of various types of dopants and their influence on the electrical properties and T_c.

In many cases, the influence of chemical doping on T_c in perovskites such as $BaTiO_3$ can be rationalized by simple ion-size effects and the changes in the tolerance factor, t.[5] For example, partial replacement of Ba^{2+} by the smaller Sr^{2+} cation on the A-site reduces the tolerance factor, and T_c decreases as the cubic polymorph is stabilized to a lower temperature. This works extremely well for the $Ba_{1-x}Sr_xTiO_3$ solid solution where T_c decreases linearly at a rate of –3.5 °C/at% Sr across the range $0 \le x \le 1$.[6] In the case of the $Ba_{1-x}Ca_xTiO_3$ solid solution ($0 \le x \le 0.24$), T_c shows anomalous behavior:[7,8] T_c initially rises with increasing x to a maximum value of ≈138 °C for $x \approx 0.08$ before decreasing to ≈118 °C at the solid solution limit of $x \approx 0.24$. The initial rise in T_c has been attributed to A-cation size variance associated with the significant size mismatch in the ionic radius of the Ba^{2+} and Ca^{2+} cations on the A-site.[8] This mismatch induces strain in the lattice and is responsible for the initial rise in T_c for Ca-doping before size-effects start to dominate for larger x. Similar cation variance effects have been reported in structural and electronic phase transitions in other perovskite-related materials.[9,10]

Trivalent rare earth ions (RE^{3+}) are commonly used at low dopant levels in commercial formulations of $BaTiO_3$-based devices to improve performance, e.g., the reliability in capacitors operating under high voltages.[1] Based on equilibrium phase diagram studies of possible RE A-site doping mechanisms, it has been established that charge compensation occurs by the creation of B-site vacancies, i.e., $Ba_{1-x}RE_xTi_{1-x/4}O_3$.[11,12] For large RE ions such as La^{3+}, an extensive solid solution occurs with $0 \le x \le 0.20$ and T_c decreases dramatically at a rate of –24 °C/at%La for $x \le 0.06$, prior to the onset of ferroelectric relaxor behavior.[12] This strong suppression of T_c has been attributed to the disruption of the ferroelectric domains due to the creation of Ti-vacancies in the TiO_3 sub-lattice (in addition to a size effect due to partial replacement of Ba with smaller La ions on the A-site).[11,13] Recently, Ben and Sinclair reported the solid solution limit for Gd-doped samples to be much smaller, $x \approx 0.05$, and T_c decreased linearly with x at a rate of –8 °C/at% Gd.[14] The lower solid solution limit for Gd- compared to La-doping is consistent with an ion size effect given the significantly smaller radius of Gd compared with La and Ba. The trend in T_c, however, is inconsistent with a simple ion size argument. Ben and Sinclair attributed the variation in T_c for Gd-doped samples to be another example of A-cation variance, in this case between Ba^{2+} and Gd^{3+} cations, and this induces local strain in the lattice that suppresses the rate of decrease in T_c. In this case, the strain effect is not sufficient to produce an increase in T_c on doping, as observed for A-site Ca-doping (up to $x \approx 0.08$), and this is presumably due to the strong influence of Ti-vacancies (V_{Ti}) in suppressing T_c in $Ba_{1-x}RE_xTi_{1-x/4}O_3$ materials.

Simulation methods offer an exciting tool for analyzing the local strain effect reported in these materials which are often inaccessible to experiment due to the low concentration of dopants and very localized atomic displacements. This provides the user with the opportunity to observe the small, sometimes

Dr. C. L. Freeman, J. A. Dawson, Prof. J. H. Harding, Dr. L.-B. Ben, Prof. D. C. Sinclair
Department of Materials Science and Engineering
University of Sheffield
Mappin St., Sheffield, S1 3JD, UK
E-mail: c.l.freeman@sheffield.ac.uk

DOI: 10.1002/adfm.201201705

subtle, local alterations that occur in the lattice.[15,16] Crucial to any classical modeling of these materials is a reliable potential set. We have recently developed a new potential set for modeling $BaTiO_3$.[17] Unlike previous potential development our model was fitted to account for the small degree of covalency that exists between Ti and O by treating these nonbonded interactions via a Lennard-Jones 7-6 potential rather than the standard Buckingham potential and adding additional three body terms. The potential is also fitted to ensure the known energetics of $BaTiO_3$ and the relevant end-members (BaO and TiO_2) are correct to ensure solution energies for defect calculations are reliable. This has proved highly successful in reproducing and explaining experimental results.[18] We now use this model to analyze in detail the local relaxations that occur in both La- and Gd-doped $BaTiO_3$ to identify the origin and result of these local strain effects.

All the simulations reported are on the cubic phase of the perovskite. It is not possible to model the tetragonal phase via classical energy minimizations as this phase is only stabilized by small dipole interactions that will not overcome the strong Coulombic interactions. The tetragonal and cubic phases are similar and the local relaxations that occur due Coulombic interactions from defects are likely to exist or be similar in both. How the defects stabilize or destabilize the tetragonal phase can also be interpreted by examining the direction of the relaxations and the energy associated by ion movements.

2. Results and Discussion

2.1. Defect Structure

The relaxed defect structure for the 4% Gd-doped $BaTiO_3$ samples are shown in **Figure 1** which exhibit the same main features as those of the La-doped samples. As can be seen the RE ions cluster in the lattice within one plane of the Ti vacancy. The same defect cluster was observed for our point defect simulations reported previously.[17] The RE cations cluster towards the V_{Ti} due to the reduced Coulombic repulsion of this site and the stronger interactions that can be generated with the surrounding oxygen anions as these are not interacting with the vacant Ti site. Lattice parameters for the La- and Gd-doped cells are listed in **Table 1**. Doping has little effect on the cell with a small increase in the cell volume with La-doping and a very small decrease with Gd-doping.

Table 1. Lattice parameters for La- and Gd-doped cells.

Parameter	undoped	La	Gd
a	4.01 Å	4.01 Å	4.01 Å
b	4.01 Å	4.01 Å	4.01 Å
c	4.01 Å	4.01 Å	4.01 Å
volume	64.30 $Å^3$	64.33 $Å^3$	64.29 $Å^3$

In considering the local structure of the defect cluster it is useful to break down the relaxations into the two defects: the V_{Ti} and the RE_{Ba} which are represented sequentially in **Figure 2**. Firstly, the creation of a V_{Ti} causes the six surrounding oxygens to be pulled towards their other neighboring Ti away from the vacancy (Figure 2a). Therefore, the Ti-O separations for these particular oxygens reduces. Secondly, the smaller size of the RE^{3+} cations, compared to the Ba, means they are unable to fully fill the 12-coordinate dodecahedral site and they move off-center toward the V_{Ti} site, as there is a smaller Coulombic repulsion here (Figure 2b). This creates several shells of RE-O separations (see **Table 2**) based primarily on ninefold coordination; 3 RE-O which are shorter than the standard Ba-O, 6 RE-O which are approximately the same separation and 3 RE-O which are significantly longer (and therefore effectively beyond the nearest neighbor shell). Thirdly, these nine neighboring oxygens around the RE cations are pulled in closer to the RE cations due to its 3+ charge (Figure 2c). This moves the oxygens out of the octahedral plane with their neighboring Ti and produces both octahedral distortion and tilting. Fourthly, the oxygens on the far side of the Ti away from the RE cations move closer towards the Ti reducing the Ti-O separation (Figure 2d) as the neighboring oxygen have been pulled away from this oxygen and towards the RE cations. The Ti also shifts towards the RE cations as it is pulled by the oxygen relaxations. The 3+ charge of the RE cations, however, limits this relaxation so it remains out of plane with its neighboring oxygen.

A similar but smaller relaxation can be observed for the Ba in the plane below the V_{Ti} which also move toward the vacancy. The smaller charge of the Ba cations means the oxygen anions do not undergo such large displacements and also the neighboring Ti is able to displace to a more central position within the octahedra.

Although the general relaxations are the same for both the La and Gd the sizes of these relaxations vary. The larger size of La compared to Gd means that it does not move as far off-center within the dodecahedron and the La-O separations are generally larger than the Gd-O separations. The distortion of the

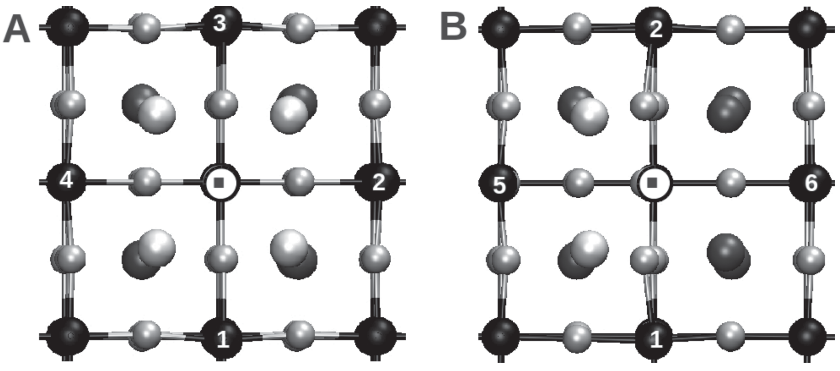

Figure 1. Relaxed defect structure for the 4% doped Gd-$BaTiO_3$ system in two different orientations: A) looking down on the plane of four Gd cations and B) looking along the plane of Gd cations. The Ti that neighbor the V_{Ti} are numerically labeled. Key: oxygen (silver), titanium (black), barium (dark grey), gadolinium (white), and V_{Ti} (circle with dot).

Adv. Funct. Mater. **2012**,
DOI: 10.1002/adfm.201201705

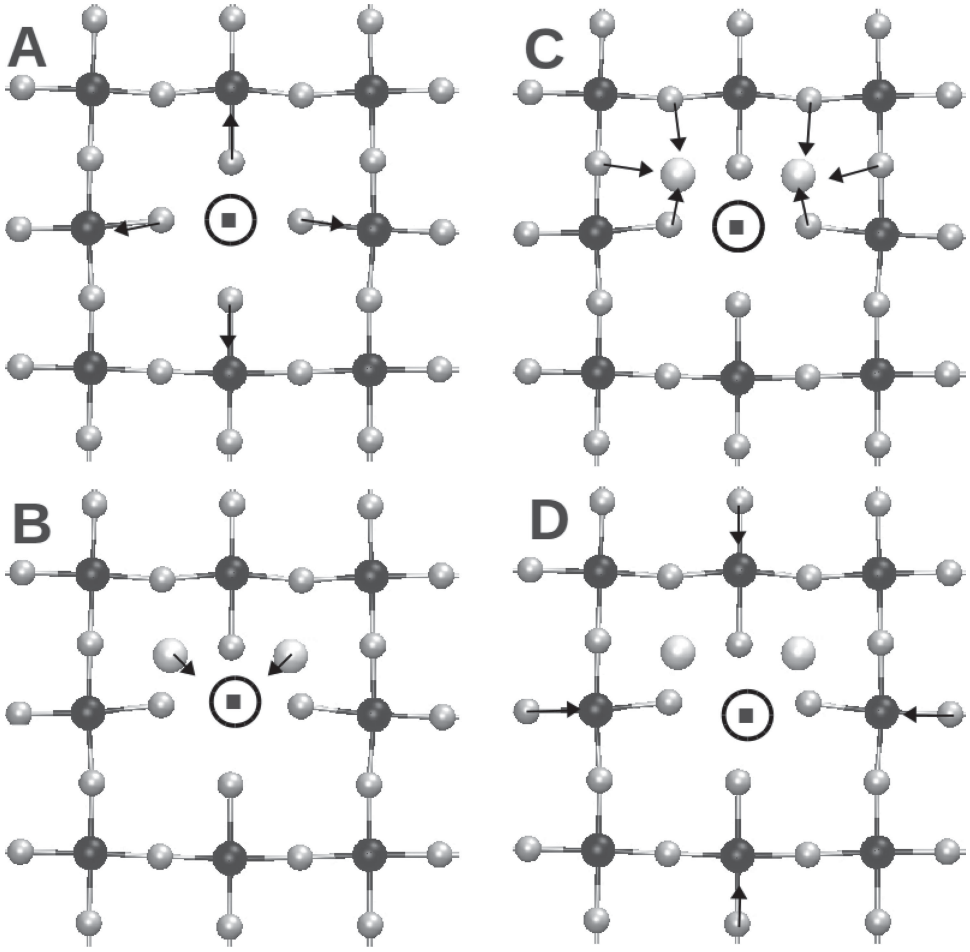

Figure 2. Relaxations of the defect site. The relaxations of particular ions are shown: A) the oxygen neighboring the V_{Ti}; B) the RE cations; C) the oxygen neighboring the RE cations; and D) the remaining oxygen that form part of the neighboring TiO_6 but are beyond the RE neighbors. Note the barium cations are not shown for clarity. Key: oxygen (silver), titanium (black), gadolinium (white) and V_{Ti} (circle with dot).

Table 2. Local coordination of the A-site cations around the V_{Ti}.

Cation	Defect	A-O
Gd	Gd	2x 2.23, 1x 2.48, 4x 2.79, 2x 2.91, 3x 3.22
Ba	Gd	1x 2.58, 2x 2.82, 2x 2.86, 4x 2.90, 2x 3.07, 1x 3.09
La	La	2x 2.38, 1x 2.58, 2x 2.80, 2x 2.85, 2x 2.89, 1x 3.10, 2x 3.12
Ba	La	1x 2.58, 2x 2.80, 2x 2.87, 2x 2.89, 2x 2.93, 2x 3.12, 1x 3.14

Table 3. Local coordination of the TiO_6 octahedra neighboring the V_{Ti}. See Figure 1 for the positions of the numbered Ti.

Dopant	Ti	Number of neighboring RE	Ti-O separations
Gd	Ti1-4	2	1x 1.92, 1x 1.96, 3x 2.00, 1x 2.01
Gd	Ti5	4	1x 1.91, 1x 1.95, 4x 2.00
Gd	Ti6	0	1x 1.91, 1x 1.96, 4x 2.01
La	Ti1-4	2	1x 1.91, 1x 1.95, 1x 2.00, 2x 2.01, 1x 2.02
La	Ti5	4	1x 1.90, 1x 1.95, 4x 2.01
La	Ti6	0	1x 1.91, 1x 1.96, 2x 2.01, 2x 2.02

Ti octahedra is largely caused by the presence of the RE cations and this controls how much the Ti is able to relax towards the RE cations following the displacement of the oxygen toward the RE cations. The more centralized position of the La within the dodecahedra compared to the Gd means the Ti relaxes less toward the La compared to the Gd case. This causes the neighboring TiO_6 to undergo a greater distortion from the ideal octahedral shape (see **Table 3** and **Figure 3**) in the La-doped system compared to the Gd-doped system.

2.2. Implications for T_c

The specific relaxations of the TiO_6 octahedra leave the Ti out of the oxygen plane in a similar manner to that observed in the tetragonal phase. Unlike the ferroelectric state, however, these relaxations are limited to the six Ti that are nearest neighbor to the V_{Ti} and the direction of the Ti moving out of plane is always away from the RE cations which means the relaxations are orthogonal or opposite to each other and not in the same direction as would be observed in the ferroelectric phase (see

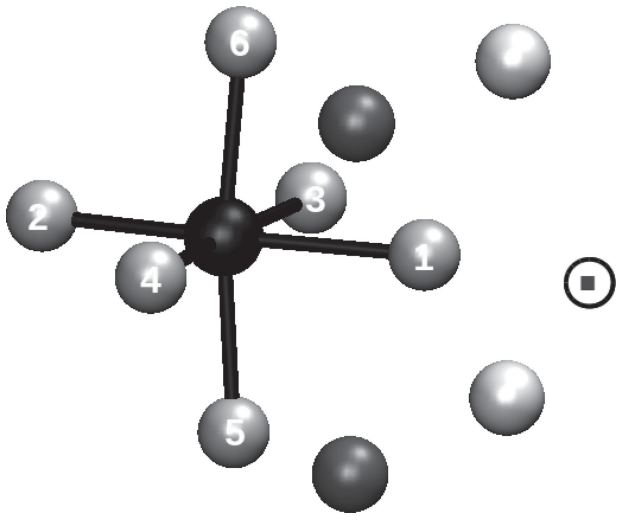

Figure 3. The structure of the TiO_6 neighboring the V_{Ti}. The oxygen atoms are numerically labeled as referenced in the text: O1 closest to the V_{Ti}, O2 furthest from V_{Ti}. Key: oxygen (silver), titanium (black), gadolinium (white), barium (dark grey) and V_{Ti} (circle with dot).

Figure 4). The relaxations induced by the defects spread further than the nearest neighbor Ti and small distortions can be seen in octahedra further from the RE cations. These relaxations also displace Ti away from the RE cations. Therefore the presence of the RE cations will destabilize the tetragonal phase as the local relaxations around these cations will disrupt the order of the Ti relaxation which need to all align, at least on a local scale, to form ferroelectric domains. When the tetragonal phase is formed within a RE-doped sample this will not be as low in energy as in undoped $BaTiO_3$ since the local coordination

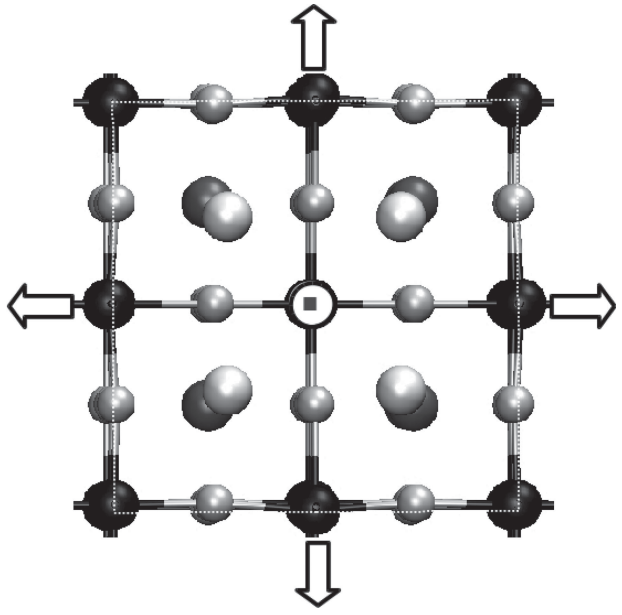

Figure 4. Dipole direction on each of the TiO_6 octahedra around the defect sites. The relaxations lead to a set of dipoles opposite and orthogonal to each other. Key: oxygen (silver), titanium (black), gadolinium (white) and V_{Ti} (circle with dot).

Table 4. Displacement of five Ti cations nearest to the RE defects within the cell as labeled in Figure 1.

Defect	Ti	Displacement in each lattice direction [Å]			Total displacement [Å]
		a	*b*	*c*	
Gd	1	0.32	0.26	0.18	0.45
Gd	2	0.32	0.26	0.34	0.53
Gd	3	0.32	0.16	0.26	0.44
Gd	4	0.32	0.36	0.26	0.55
Gd	5	0.36	0.26	0.26	0.51
La	1	0.26	0.20	0.11	0.35
La	2	0.26	0.20	0.30	0.44
La	3	0.26	0.10	0.21	0.35
La	4	0.26	0.31	0.21	0.46
La	5	0.35	0.20	0.21	0.45

around the RE cations will not be optimal for the Coulombic interactions: smaller thermal vibrations will be necessary to convert the tetragonal phase into the cubic phase. The observed drop in T_c with doping of RE cations on the A-site of $BaTiO_3$ based on experimental results[12,14] is therefore entirely consistent with our simulations.

It is now important to consider the differences between La- and Gd-doping. The size of the relaxations for the five Ti nearest the rare-earth cations are listed in **Table 4** for both the La- and Gd-doped systems. As can be seen the Ti relax less in the La- (average 0.41 Å) compared to Gd-doped system (average 0.50 Å) which is due to the position of the La cation which sits more centrally within the dodecahedron than the Gd cation. This prevents the Ti moving as far towards the V_{Ti} in the La- compared to Gd-doped system. **Figure 5** shows the energy change for displacing the Ti directly toward the center of the TiO_6 octahedra and therefore towards the RE cations for the three different neighbor Ti sites in the Gd-and La-doped systems. For Ti 1-5 the energy well for the Ti is deeper in the La-doped system due

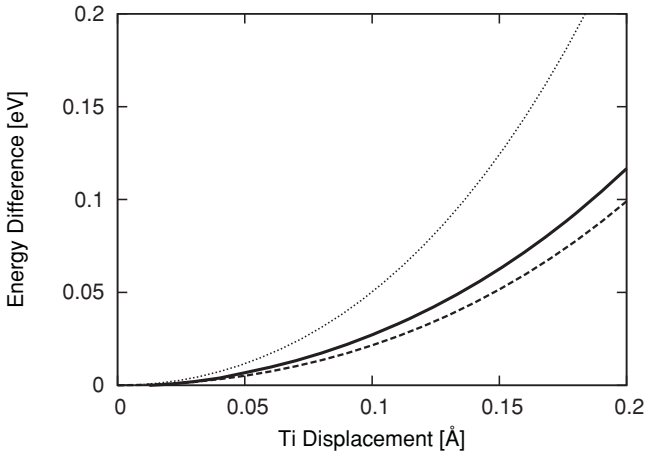

Figure 5. Difference in the energy change with displacing the Ti that neighbor the V_{Ti} toward the vacancy for the La- minus the Gd-doped systems. Plotted for the Ti that neighbor two RE cations (Ti1-4) (dotted line), four RE cations (Ti5) (solid line) and no RE cations (Ti6) (dashed line).

DOI: 10.1002/adfm.201201705

to the greater repulsion the La cation causes for the Ti compared to Gd. This implies there is a stronger energetic preference for the Ti to be shifted off-centre within the octahedra in the La system compared to the Gd system. Given the La-doped system is harder to energetically displace toward the necessary position for the tetragonal phase we can infer there will be a smaller energy barrier towards converting the tetragonal phase to the cubic. Therefore smaller thermal vibrations are required in the La-doped system to convert it from the tetragonal to the cubic phase compared to the Gd-doped system. This explains the lower T_c reported for La-doped samples based on experimental results.[14]

3. Conclusions

Experimental work has suggested that a local strain effect must be responsible for the unusual behavior of T_c with RE-doping in $BaTiO_3$ where the T_c lowers at a greater rate with the larger La cation compared to the smaller Gd cation.[14] Using classical lattice minimization simulations we are able to identify the defect structure and analyze the local relaxations that cause this strain. Our simulations demonstrate that both RE cations induce similar relaxations that result in the surrounding TiO_6 octahedra distorting in a similar manner to that of the tetragonal phase but with none of the necessary dipole alignment. This relaxation will disrupt the tetragonal phase lowering the temperature at which conversion to the cubic phase occurs. The relaxations are more significant in the case of the La cation due to the larger size of the La cation which remains more centrally located within the dodecahedral A-site compared to the smaller Gd cation. As a consequence, the La causes T_c to decrease more than Gd. Classical simulations using our new potential model provide an ideal method to explore these complex local atomic scale relaxations that are responsible for much of the unique chemistry in these materials.

4. Methods

Lattice minimization simulations were performed with the General Utility Lattice Program (GULP)[19] using potentials we have developed[17] for $BaTiO_3$ and those of Lewis and Catlow[20] for La and Gd which are compatible with our potential model. La and Gd were doped into a supercell of 100 formula units of $BaTiO_3$ to reach the experimental defect concentrations reported (≈4%). Previous simulations[17] and experiments[21,2] have shown that A-site substitution by RE cations results exclusively in the creation of Ti vacancies and therefore we only consider this compensation mechanism in our simulations.

It is important to identify the low energy configurations within the vast array of potential configurations that exist for a large supercell. We employed a genetic algorithm (GA) approach to configurational sampling. This operated by beginning with twenty configurations where the four RE cations and Ti vacancy were randomly distributed. Single point energies were calculated for these configurations and then the configurations were ordered by their lattice energy. Configurations had a 50% chance of being selected starting with the lowest energy configuration and working up the list. Once two configurations were selected the positions of their defects were randomly mixed to generate a new configuration. This procedure was repeated until twenty new configurations had been selected and a new breeding round was initiated. A total of forty breeding rounds were conducted and four GA runs were attempted. From these four GA runs the final lowest energy configurations were used as starting points for a subsequent set of four GA runs using an identical procedure with the exception that full optimizations were now performed on the configurations rather than only single point calculations. To ensure diversity in the population it is important to include the potential for mutation. For each configuration there was a 10% chance of a mutation where one defect site was randomly moved within the lattice. From these runs the final lowest energy configuration was identified and is reported here.

Acknowledgements

This work was supported by the Engineering and Physical Sciences Research Council (Grant number EP/G005001/1).

Received: June 22, 2012
Revised: August 14, 2012
Published online:

[1] H. Kishi, Y. Mizuno, H. Chazono, *Jpn. J. Appl. Phys., Part 1* **2003**, *42*, 1.
[2] F. D. Morrison, D. C. Sinclair, A. R. West, *J. Am. Ceram. Soc.* **2001**, *84*, 474.
[3] J. F. Ihlefeld, W. J. Borland, J.-P. Maria, *Adv. Funct. Mater.* **2007**, *17*, 1199.
[4] B. Jaffe, W. R. Cook, H. Jaffe, *Piezoelectric Ceramics,* Academic Press, New York **1971**.
[5] V. M. Goldschmidt, *Naturwissenschaften* **1926**, *14*, 477.
[6] A. J. Moulson, J. M. Herbert, *Electroceramics - Materials, Properties, Applications,* John Wiley and Sons, New York **2003**.
[7] T. Mitsui, W. B. Westphal, *Phys. Rev.* **1961**, *124*, 1354.
[8] D. C. Sinclair, J. P. Attfield, *Chem. Commun.* **1999**, *16*, 1497.
[9] J. P. Attfield, A. L. Kharlanov, J. A. McAllister, *Nature* **1998**, *394*, 157.
[10] J. P. Attfield, *Chem. Mater.* **1998**, *10*, 3239.
[11] D. Makovec, Z. Samardzija, U. Delalut, D. Kolar, *J. Am. Ceram. Soc.* **1995**, *78*, 2193.
[12] F. D. Morrison, D. C. Sinclair, A. R. West, *J. Appl. Phys.* **1999**, *86*, 6355.
[13] F. D. Morrison, D. C. Sinclair, J. M. S. Skakle, A. R. West, *J. Am. Ceram. Soc.* **1998**, *81*, 1957.
[14] L.-B. Ben, D. C. Sinclair, *Appl. Phys. Lett.* **2011**, *98*, 092907.
[15] G. C. Mather, M. S. Islam, F. M. Figueiredo, *Adv. Funct. Mater.* **2007**, *17*, 905.
[16] C. L. Freeman, N. L. Allan, W. van Westrenen, *Phys. Rev. B* **2006**, *74*, 13.
[17] C. L. Freeman, J. A. Dawson, H.-R. Chen, J. H. Harding, L.-B. Ben, D. C. Sinclair, *J. Mater. Chem.* **2011**, *21*, 4861.
[18] J. A. Dawson, C. L. Freeman, L.-B. Ben, J. H. Harding, D. C. Sinclair, *J. Appl. Phys.* **2011**, *109*, 0842102.
[19] J. D. Gale, A. L. Rohl, *Mol. Simul.* **2003**, *29*, 291.
[20] G. V. Lewis, C. R. A. Catlow, *J. Phys. C: Solid State Phys.* **1985**, *18*, 1149.
[21] F. D. Morrison, A. Coats, D. C. Sinclair, A. R. West, *J. Electroceram.* **2001**, *6*, 219.